



**METABOLIC, ENDOCRINE, AND GENITOURINARY PATHOBIOLOGY**

# Chronic Exposure to Palmitic Acid Down-Regulates AKT in Beta-Cells through Activation of mTOR



Richa Aggarwal,\* Zhechu Peng,\* Ni Zeng,\* Joshua Silva,\* Lina He,\* Jingyu Chen,\* Anketse Debebe,\* Taojian Tu,\*  
Mario Alba,\* Chien-Yu Chen,\* Eileen X. Stiles,\* Handan Hong,\* and Bangyan L. Stiles\*<sup>†</sup>

From the Department of Pharmacology and Pharmaceutical Sciences,\* School of Pharmacy, and the Department of Pathology,<sup>†</sup> Keck School of Medicine, University of Southern California, Los Angeles, California

Accepted for publication  
September 22, 2021.

Address correspondence to  
Bangyan L. Stiles, Ph.D.,  
Department of Pharmacology  
and Pharmaceutical Sciences,  
School of Pharmacy, University  
of Southern California, Los  
Angeles, CA 90033. E-mail:  
[bstiles@usc.edu](mailto:bstiles@usc.edu).

High circulating lipids occurring in obese individuals and insulin-resistant patients are considered a contributing factor to type 2 diabetes. Exposure to high lipid concentration is proposed to both protect and damage beta-cells under different circumstances. Here, by feeding mice a high-fat diet (HFD) for 2 weeks to up to 14 months, the study showed that HFD initially causes the beta-cells to expand in population, whereas long-term exposure to HFD is associated with failure of beta-cells and the inability of animals to respond to glucose challenge. To prevent the failure of beta-cells and the development of type 2 diabetes, the molecular mechanisms that underlie this biphasic response of beta-cells to lipid exposure were explored. Using palmitic acid (PA) in cultured beta-cells and islets, the study demonstrated that chronic exposure to lipids leads to reduced viability and inhibition of cell cycle progression concurrent with down-regulation of a pro-growth/survival kinase AKT, independent of glucose. This AKT down-regulation by PA is correlated with the induction of mTOR/S6K activity. Inhibiting mTOR activity with rapamycin induced Raptor and restored AKT activity, allowing beta-cells to gain proliferation capacity that was lost after HFD exposure. In summary, a novel mechanism in which lipid exposure may cause the dipole effects on beta-cell growth was elucidated, where mTOR acts as a lipid sensor. These mechanisms can be novel targets for future therapeutic developments. (*Am J Pathol* 2022, 192: 130–145; <https://doi.org/10.1016/j.ajpath.2021.09.008>)

Macronutrients are recognized as factors that not only supply energy but also alter cellular growth response. These effects of glucose and lipids are particularly relevant to the function of pancreatic beta-cells because they respond to changes in plasma glucose and lipid levels to regulate insulin release. In individuals with normal blood glucose levels, this increased insulin requirement is met by increased insulin secretion from pancreatic beta-cells. In patients with diabetes, the beta-cells are unable to meet the increased insulin demands, and patients manifest increasing glucose levels (hyperglycemia) and ultimately type II diabetes (T2D).<sup>1–6</sup>

Two factors contribute to the inability of beta-cells to compensate for the demand of hyperglycemia occurring in T2D: loss or reduction of the ability for beta-cells to secrete insulin; and reduction of the number of beta-cells.<sup>2,5,7</sup>

Hyperglycemia and hyperlipidemia, the two conditions that hallmark insulin resistance, have both been hypothesized to regulate insulin secretion and the growth/survival of beta-cells.<sup>7</sup> Glucose is known to stimulate beta-cell insulin secretion through regulation of the ATP-potassium transporter. It also stimulates the growth of beta-cells by regulating cyclin D2 expression.<sup>8,9</sup> Compared with those of glucose, the effects of lipids are less clear. Depending on the type of lipid or duration of exposure, fatty acids can both stimulate or inhibit the function and growth/survival of cultured cells.<sup>10–14</sup> Cultured human islets exposed to

Supported by NIH grants R01DK084241 (B.L.S.), the USC Center for Liver Disease grant P30DK48522 (B.L.S.), and National Cancer Institute grant R01CA154986 (B.L.S.).

Disclosures: None declared.

palmitic acid (PA) for 4 days lead to apoptosis of beta-cells, whereas oleic acid protects against PA and glucose-induced beta-cell death.<sup>11</sup> Similarly, prolonged exposure of rat or mouse islets to free fatty acids causes decreased insulin transcription, impair glucose-induced insulin secretion, and finally, result in beta-cell apoptosis.<sup>10,15–18</sup> However, increased beta-cell function and proliferation have also been reported when islets or beta-cells are exposed to free fatty acids.<sup>19–21</sup> Overall, it appears that whereas short-term exposure to free fatty acids is pro-growth, long-term exposure is deleterious for the beta-cells.

Several growth factors have been found to play roles in beta-cell function, including insulin, insulin-like growth factor (IGF), and hepatic growth factor (HGF).<sup>22–28</sup> These studies suggest that the PI3K/AKT pathway plays a mitogenic role in beta-cell growth because IGF-1, insulin, and HGF signal through the PI3K/AKT signaling pathway.<sup>29–32</sup> Consistently, genetic studies manipulating AKT and PTEN (phosphatase and tensin homologue deleted on chromosome 10), the negative regulator of PI3K/AKT signal, confirm the role of PI3K/AKT in beta-cell growth and survival.<sup>31,33–37</sup> One primary consequence of AKT activation is the induction of mTOR activity, the role of which in beta-cell growth and function are context-dependent.<sup>38–41</sup> Although metabolic regulation of mTOR by nutrients may play a role in the context-dependent role of mTOR,<sup>42</sup> the feedback regulation of mTOR target on AKT signal may also play a role. Ribosomal S6 kinase (p70S6K1), a substrate phosphorylated by mTOR kinase, induces the phosphorylation and degradation of insulin receptor substrate 1 (IRS1),<sup>43,44</sup> thus inhibiting the PI3K/AKT signal.

This study comprehensively evaluated the effect of short-term and chronic HFD feeding on islet mass and beta-cell proliferation. The results work demonstrated a clear biphasic effect of HFD feeding on beta-cell growth/survival. The study then focused on the effects of the saturated fatty acid PA on beta-cell growth and survival. The results indicated that prolonged exposure of beta-cells to PA treatment caused suppressed proliferation and induced apoptosis, concurrent with inhibition of AKT activity, whereas short-term exposure induced the pro-growth and pro-survival kinase AKT. The mechanisms by which chronic exposure to PA suppresses AKT activity were further elucidated, and a role of mTOR/Raptor-mediated S6K activity in the regulation of AKT by PA was observed.

## Materials and Methods

### Animals

Mice of mixed backgrounds were used for the high-fat diet (HFD) studies because different backgrounds have been shown to have different responses to HFD. The use of mice with mixed genetic backgrounds allows assessment in non-homogeneous populations. All animals were housed in a temperature-, humidity-, and light-controlled room

(12-hour light/dark cycle), allowing free access to food and water. All experiments were conducted according to the Institutional Animal Care and Use Committee of the University of Southern California research guidelines.

### Cell Culture

Various beta-cell lines (bTC6, MIN-6, and INS-1) and non-beta-cell lines [mouse embryonic fibroblasts (mEFs)] were used for the study. INS-1 cells were kindly supplied by Prasanna Dadi at Vanderbilt University. All cells were cultured at 37°C in a humidified atmosphere containing 5% CO<sub>2</sub> in either Dulbecco's modified Eagle's medium containing 25 mmol/L glucose or RPMI 1640 medium containing 11 mmol/L glucose and supplemented with 10% heat-inactivated fetal bovine serum, 50 μmol/L 2-mercaptoethanol, 100 U/mL penicillin, and 100 μg/mL streptomycin. Cells were starved overnight 48 hours after seeding and then treated with 0.4 mmol/L PA in media containing 2, 6, or 15 mmol/L glucose as indicated. All screening experiments performed with mEFs were done multiple times with different combinations of dose, time, and glucose concentration. All beta-cell experiments were performed at least three times for replication.

### Diet Feeding

For the HFD experiment, one group of mice was fed with HFD with 60 kcal% fat (TD06414; Harlan Laboratories, Indianapolis, IN), whereas the control group was fed with normal chow (NC) with 13 kcal% of fat in their diet (PicoLab 5053; Northlake, TX).<sup>45–47</sup> Diet was started at 3 months of age and continued for the indicated period of time. Body weight, food intake, and random plasma glucose levels were monitored weekly. Bromo 5-bromo-2'-deoxyuridine (BrdU; 1 mg/mL in deionized water; BD Pharmingen, San Diego, CA) was given to mice in water for 5 days before the end of the study.<sup>47</sup> Pancreases were collected at the end of the 5 days following overnight fasting.

### Biochemical Analysis

Glucose tolerant tests were performed on 16-hour-fasted mice by i.p. injection of 30% glucose. Glucose levels were tested using blood from tail vein puncture,<sup>48</sup> and the area under curve was calculated. Plasma samples were also collected through cardiac puncture at the end of the study following overnight fasting. A Mouse Ultrasensitive Insulin ELISA kit from ALPCO (Cat#80-INSMSU-E01; ALPCO, Salem, NH) was used for quantifying plasma insulin per kit instructions as described previously.<sup>36,37</sup>

### Mouse Islet Isolation

Pancreases were perfused with collagenase P solution (0.8 mg/mL; 5 mL per mouse) and digested at 37°C for 17

minutes. Islets were then purified by using Ficoll gradients with densities of 1.108, 1.096, 1.069, and 1.037 (Cellgro Technologies, Lincoln, NE) as previously reported.<sup>36,37</sup> Islets between layer 1.096 and 1.069 were collected and handpicked for either protein extraction or RNA extraction.<sup>37,49</sup>

### Rapamycin Treatment in Mice

Mice were fed with HFD for the required duration, and rapamycin was injected intraperitoneally on the last 8 days of treatment (0.3 mg/kg per mouse per day). Rapamycin stock (100 mmol/L) in dimethyl sulfoxide (#R-5000; LC Laboratories, Woburn, MA) was diluted 100-fold by mixing 890  $\mu$ L of phosphate-buffered saline, 100  $\mu$ L of Tween 80, and 10  $\mu$ L of rapamycin stock. Calculations were then made, and mice were injected as per their body weight.

### Immunohistochemistry

At the end of the study, pancreases were dissected *en total* and fixed in Zn-formalin at 4°C for histopathology and immunohistochemistry analysis. Zn-formalin-fixed and paraffin-embedded sections were stained with hematoxylin and eosin for histopathology analysis.<sup>27,50</sup> Islet mass was calculated based on area of islets versus total pancreas area measurement collection from three sections per sample 60  $\mu$ mol/L apart as described.<sup>36,49</sup>

Pancreas sections were also stained with antibodies for immunohistochemical or immunofluorescence analysis. Antibodies used were cyclin D2 (sc-593; Santa Cruz Biotechnology, Dallas, TX), Ki-67 monoclonal antibody (CST#12202), and BrdU (BD Pharmingen). A terminal deoxynucleotidyl transferase-mediated dUTP nick-end labeling (TUNEL) kit from BD Pharmingen was used for assessment of apoptotic cells following the manufacturer's instructions as described.<sup>33,51</sup> Ki-67 and BrdU staining was scored using Zeiss Axiovision 4.8 software (Zeiss, Oberkochen, Germany). TUNEL-stained islets were quantified using NIH ImageJ software version 2.0 (NIH, Bethesda, MD; <https://imagej.nih.gov>) with Fiji and Cell Profiler for total nuclei, and TUNEL-positive nuclei were counted manually. All islets from each mouse pancreas were counted.

### Fatty Acid Preparation

PA (sigma#P0500-10G; Sigma-Aldrich St. Louis, MO) 200 mmol/L stock was prepared by dissolving 51.2 mg of PA in 1 mL of 100% ethanol; 0.04 mL of this stock was further dissolved in 1.96 mL of 10% fatty acid-free bovine serum albumin (BSA; in Dulbecco's modified Eagle's medium) for 4 mmol/L PA stock by shaking overnight at room temperature. On the following day, the solution was filtered through a 0.22  $\mu$ mol/L filter and

diluted 1:10 with medium prior to cell treatment. One percent BSA in Dulbecco's modified Eagle's medium was used as a control.

### MTT Assay

Cells were seeded at density 1.5 to 2  $\times$  10<sup>4</sup> cells/well in 96-well plates in RPMI medium. After 48 hours of seeding, the cells were either treated with 1% BSA (as control) or different concentrations of PA (0.2 mmol/L, 0.4 mmol/L, 0.6 mmol/L, 0.8 mmol/L, and 1 mmol/L; six wells per treatment) and incubated for 24 or 48 hours. MTT reagent (10  $\mu$ L) was then added after respective incubation and kept at 37°C for 4 hours, followed by addition of 100  $\mu$ L of dimethyl sulfoxide. The plate was kept on the shaker for 5 to 10 minutes to dissolve the crystals. Optical density reading was then taken at 570-nm wavelength.<sup>52</sup>

### Cell Cycle Fluorescence-Activated Cell Sorting

INS-1 cells (3  $\times$  10<sup>5</sup> cells/well) were seeded in six-well plates in RPMI medium with 6 mmol/L glucose with 10% fetal bovine serum. Cells were starved for 48 to 72 hours in medium without fetal bovine serum after 24 hours of seeding. They were then treated with 1% BSA or 0.4 mmol/L PA for 48 hours. Cells were harvested by washing, trypsinizing, and then centrifuging them. The resulting pellet was resuspended in 0.1 mL of phosphate-buffered saline. Cold ethanol (1 mL) was then added and kept for 20 minutes at -20°C. Cells were centrifuged at approximately 250  $\times$  g for 5 minutes, and supernatant was discarded. The pellet was then resuspended in 500  $\mu$ L of RNase solution (200  $\mu$ g/mL in phosphate-buffered saline) and incubated at room temperature for 30 minutes. Propidium iodide was later added to the mix (50  $\mu$ g/mL) and incubated for 30 minutes away from light. Fluorescence-activated cell sorting analysis was performed using a FACScalibur flow cytometer and software version 6.0 (BD Biosciences, Franklin Lakes, NJ).

### Propidium Iodide/Annexin V Fluorescence-Activated Cell Sorting

INS-1 cells were seeded at density (2.5  $\times$  10<sup>5</sup> cells/well) in six-well plates in RPMI medium. After 48 hours of seeding, cells were treated with 1% BSA or 0.4 mmol/L PA for 48 hours. Medium containing detached and floating cells was collected, and the rest of the cells were trypsinized and then washed once with phosphate-buffered saline. Cells were then washed and suspended in 1  $\times$  Annexin Binding Buffer (400 ng per 1  $\times$  10<sup>6</sup> cells) and incubated for 8 minutes at room temperature away from light. Propidium iodide was then added to each sample (2.5  $\mu$ g/mL per sample) and incubated for approximately 2 minutes. Fluorescence-activated

cell sorting analysis was then performed as previously described.<sup>53</sup>

### Immunoblotting

Cell lysate preparation and immunoblot analysis were performed as described.<sup>54,55</sup> Briefly, cells or islets were lysed in cell lysis buffer containing 1 mmol/L sodium pyrophosphate, 10 mmol/L  $\beta$ -glycerol phosphate, 10 mmol/L sodium fluoride, 0.5 mmol/L sodium orthovanadate, 1  $\mu$ mol/L microcystin, and protease inhibitor cocktail set II (Calbiochem, San Diego, CA) (36,37). Supernatants of the lysates were subjected to SDS-PAGE (10% to 12% polyacrylamide gel) and then transferred to polyvinylidene difluoride membranes. Antibodies used were phospho-AKT (Ser473; #4060; Cell Signaling Technology, Danvers, MA), phospho-p70 S6 kinase (Thr389; #9205; Cell Signaling Technology), cleaved caspase-3 (Asp175; #9661; Cell Signaling Technology), cyclin D1 (sc-8396; Santa Cruz Biotechnology), cyclin D2 (sc-593; Santa Cruz Biotechnology), p-mTOR (Ser 2448; #5536; Cell Signaling Technology), p-IRS (Ser 1101; #2385; Cell Signaling Technology), and Raptor (48648; Cell Signaling Technology). Enhanced chemiluminescence secondary mouse and rabbit horseradish peroxidase antibodies used were from GE Healthcare (Chicago, IL). Immunoblots were repeated for each sample. Densitometry was performed using ImageJ software (version 2.0) analysis.

### RNA Sequencing and Data Analysis

Six mouse islet preparations (three in the NC group and three in the HFD group, on diet for 4 months) were sequenced, and data were analyzed using Partek Flow and Ingenuity Pathway Analysis.<sup>49</sup> In brief, an RNeasy Mini Kit (Cat# 74104; Qiagen, Hilden, Germany) was used to isolate total RNA from mouse islets. RNA quality was tested using Agilent Bioanalyzer (Agilent Technologies, Santa Clara, CA), and the RNA integrity number values for all the samples were  $>7.5$ . The authors utilized University of Southern California Molecular Genetics Core for next generation sequencing services to convert mRNA to cDNA libraries, which were further sequenced using Illumina NextSeq 500 (Illumina, San Diego, CA) at 25 million reads per sample.

### Statistical Analysis

The data are presented as means  $\pm$  SEM. Differences between HFD- or PA-treated groups versus controls were analyzed by *t*-test, with two-tailed  $P < 0.05$  considered statistically significant. All tissue culture experiments were performed at least three times.

## Results

### Chronic Exposure to HFD Leads to Reduced Beta-Cell Proliferation and Induced Beta-Cell Death

HFD is a lipid-rich diet that is often used as an experimental approach to induce hyperglycemia and insulin resistance.<sup>4,6</sup> During HFD feeding, the mass of pancreatic islets increases to compensate for the demand of insulin. It is hypothesized that this increased demand for insulin production leads to beta-cell death and development of diabetes. In the current study, this HFD-induced compensatory beta-cell growth response was used as a model to explore the *in vivo* effects of hyperlipidemia on cell growth and survival. Three-month-old mice were subjected to HFD feeding for different durations ranging from 7 days to 14 months. Seven- or 15-day feeding of HFD did not significantly alter the plasma insulin levels (Figure 1A). Consistent with previous reports,<sup>12</sup> HFD feeding for 2 months was sufficient to increase fasting plasma insulin. Insulin levels peaked at 4 months, reaching approximately 10-fold induction as compared to those in the NC-fed mice. This induction was significantly diminished with 14-month HFD feeding where only a threefold induction was observed (Figure 1A). This diminished insulin response was concurrent with the development of glucose intolerance in the 14-month HFD-fed mice, where the area under curve for the glucose tolerant test was significantly higher ( $P < 0.05$ ) at  $3.26 \pm 0.24$  versus  $2.05 \pm 0.17$  in the NC-fed mice. The mice, however, did not develop overt diabetes because fasting glucose levels were comparable between the HFD ( $126 \pm 4.8$  mg/dL) and the NC ( $110 \pm 6$  mg/dL) mice. Together with the significantly elevated insulin secretion and islet mass, these data indicate that the insulin level in the HFD-fed mice is still able to compensate for the insulin resistance even though islet proliferation has started to diminish. The length of HFD needed to eventually induce sufficiently diminished insulin output/islet mass for diabetes is unclear. The mass of islets also increased concurrent with the elevated plasma insulin levels. Starting at 2 months after the start of HFD feeding, a  $1.92 \pm 0.25$ -fold induction of islet mass was observed with HFD feeding versus NC, reaching significance ( $P < 0.05$ ) at 4 month feeding. Islet mass peaked at 9 months with an approximately fourfold induction and started to decline with 14 months of HFD feeding (Figure 1A).

Proliferation of beta-cells in response to HFD feeding was assessed. The data suggest that increases in proliferation of beta-cells preceded the increase of either islet mass or plasma insulin concentration. Measured using Ki-67/BrdU staining, the data showed that 14 days of feeding of HFD is sufficient to induce beta-cell proliferation by threefold. Two-month HFD feeding induced beta-cell proliferation by nearly 10-fold (Figure 1A). Although longer feeding for 4 and 9 months continuously induced beta-cell proliferation, such induction occurred at approximately twofold or less, significantly lower than the 10-fold observed with 2 months

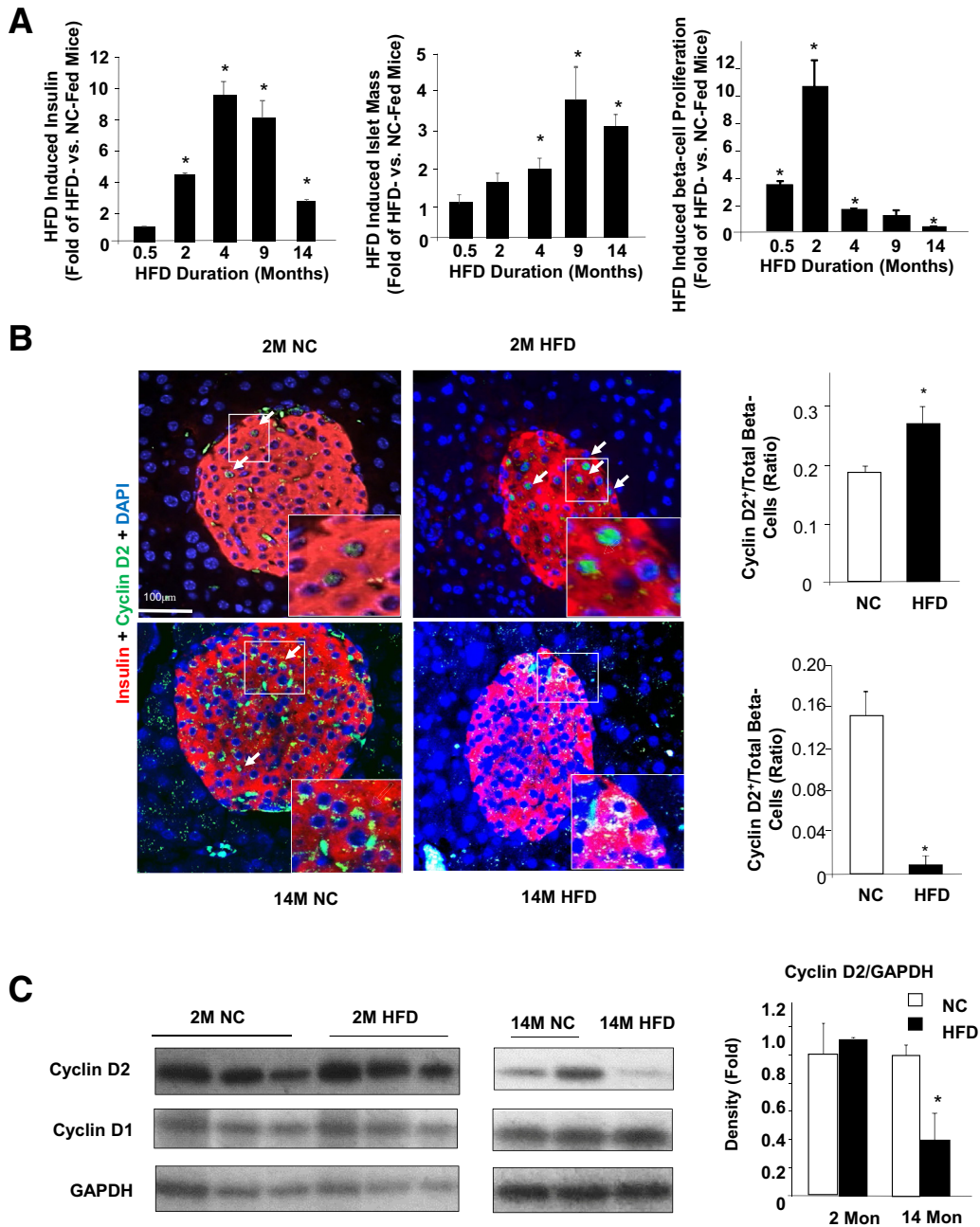


**Figure 1** High-fat diet–induced beta-cell proliferation. **A:** Three-month–old mice were put on a high-fat diet (HFD) for the indicated durations (x axes). Fold change of fasting insulin (left), islet mass (middle), and cell proliferation rate (right) were observed for HFD- versus normal chow (NC)-fed animals. **B:** Immunofluorescent staining of cyclin D2 and insulin in pancreas of HFD- and NC-fed mice. **Top panels,** mice fed on indicated diet for 2 months (2M); **bottom panels,** mice fed on indicated diet for 14 months (14M). **Right panels,** quantification of cyclin D2–positive beta-cells versus total beta-cells. Green, cyclin D2; red, insulin; blue, DAPI. **Arrows** point to the cyclin D2–positive beta-cells. **Insets** are the magnified (by two- to threefold) images of the boxed areas. **C:** Immunoblotting analysis for cyclins D1 and D2. **Left panel,** mice fed on indicated diet for 2 months (2M); **middle panel,** mice fed on indicated diet for 14 months (14M); **right panel,** densitometry quantification of the ratio of cyclin D2/GAPDH from different immunoblotting performed with isolated islets. Each lane represents one mouse. *n* = 5 to 9 mice per condition (**A**); **B** and **C:** *n* = 3 2Mon, *n* = 4 14Mon. \**P* < 0.05 compared to NC-fed mice. Scale bar = 100 μm.

of HFD feeding. By 14 months of HFD feeding, the beta-cell proliferation rate was significantly lower in the HFD-fed mice. Approximately 50% beta-cell proliferation rate was observed in the HFD feeding group versus that in the control group. The cell proliferation rate was corroborated by cyclin D2 staining where 2-month HFD feeding

significantly induced the number of cells that stained positive for cyclin D2 (Figure 1B). In the 14-month–old mice, beta-cells positive for cyclin D2 were rare in the NC (control) group and essentially undetectable in the HFD group (Figure 1B). Immunoblotting analysis of cyclin D2 confirmed that 14-month HFD feeding led to significantly

reduced expression of cyclin D2, whereas 2-month HFD increased levels of cyclin D2 in mouse islets (Figure 1C).

Apoptosis was evaluated in the beta-cells from the different HFD feeding groups using the TUNEL assay. TUNEL-positive cells were barely detectable in either the NC or the HFD-fed mice (Figure 2 and data not shown). Although TUNEL-positive cells were still rare in the 14-month HFD-fed mice, some TUNEL-positive cells were detected. In particular, some islets in the HFD group appeared to be undergoing more severe apoptosis than the control group even though the overall apoptotic rate was still very low (Figure 2). Nonetheless, the increase in cell death in response to chronic lipid exposure likely contributed to the decline of insulin levels and islet mass associated with HFD feeding. Together, these *in vivo* analyses demonstrate a two-phased response of beta-cells to HFD feeding, where short exposure induces proliferation and overall islet function, and longer exposure leads to apoptosis or cell death.

### Prolonged Exposure to PA Leads to Reduced Beta-Cell Growth/Survival

To understand this two-phased response to lipid exposure, time- and dose-dependent exposure studies to PA were performed and cell viability was evaluated using MTT assay in mEFs. The 0.4 mmol/L PA treatment induced an approximately 50% reduction in MTT in 24 hours, whereas 48-hour treatment induced further reduction (Figure 3). Similarly, 48-hour treatment was needed for 0.4 mmol/L PA to decrease cell growth/viability in beta-cells (INS-1, b-TC6, and MIN6) (Figure 3). Increasing the concentration of PA dose-dependently decreased cell growth/viability in mEFs as indicated by reduced MTT. In beta-cells, increasing concentration of PA up to 1 mmol/L had minimal additional effects, though a mild dosage effect was observed in INS-1 cells. Using the mEF cells as a model, the cell growth signals were evaluated up to 24 hours with 0.4 mmol/L of PA treatment. The data show that PA indeed induced the expression of G1 cyclins, cyclin D2, similar to that observed *in vivo* (Figure 4A). Eighteen-hour and 24-hour treatments also induced the expression of cyclin D1 at physiological range of glucose. The induction of cyclin D2 by PA, however, appears to be independent of the glucose concentrations, though the specific exposure time needed does vary with different glucose concentrations.

Surprisingly, a down-regulation of phospho-AKT was observed under all glucose conditions, particularly with 18- and 24-hour PA treatment. This observation was confirmed in the three beta-cell lines (Figure 4B). Similar to mEFs, exposure to PA for 48 hours led to reduced phospho-AKT and up-regulation of G1 cyclins including cyclin D1, D2, and A. In addition, isolated islets were exposed to PA treatment and similar down-regulation of phospho-AKT concurrent with induction of cyclin D2 was observed (Figure 4C). Furthermore, islets from HFD-fed mice also

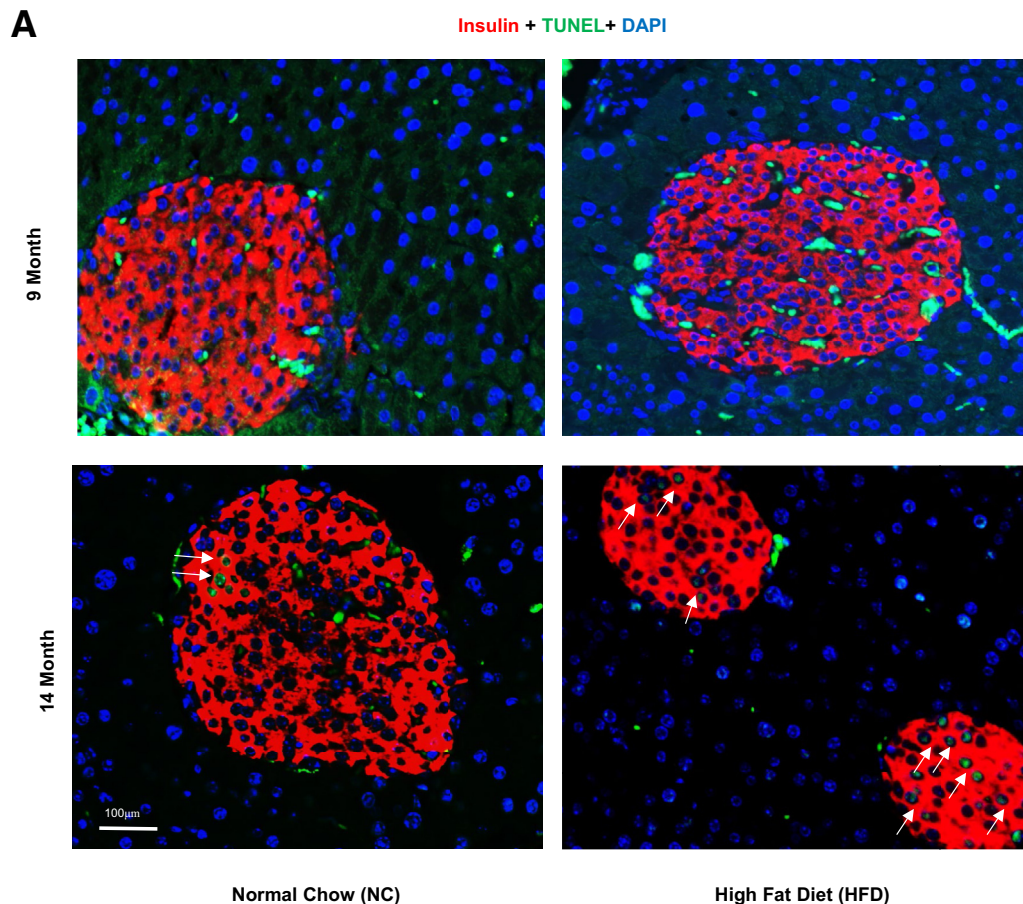
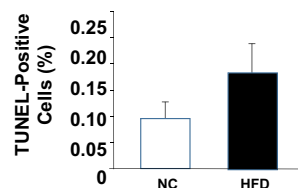
displayed similar down-regulation of phospho-AKT with induction of cyclin D2, though not as profound, likely due to mouse-to-mouse variations (Figure 4C). The down-regulation of phospho-AKT is counterintuitive to the elevated G1 cyclins because AKT is a pro-growth and pro-survival kinase. We hypothesized that the down-regulation of phospho-AKT may be a result of chronic exposure to PA, whereas short exposure would induce the phosphorylation of AKT. To address the dynamics of AKT phosphorylation in response to lipid exposure, the study assessed AKT phosphorylation in INS-1 cells treated with 0.4 mmol/L PA for 30 minutes, 4 hours, and 24 hours (Figure 5A). The results clearly indicate that short treatment for 30 minutes indeed induced AKT phosphorylation, whereas this phosphorylation was gradually lost with longer PA exposure. Twenty-four-hour exposure to PA led to down-regulation of phospho-AKT, whereas 4 hour exposure did not alter the phosphorylation of AKT.

We hypothesized that the down-regulation of AKT in response to long PA exposure may have been responsible for the loss of proliferation and increased apoptosis associated with prolonged lipid exposure. Consistent with this hypothesis, fourfold fewer cells were observed in S phase in the 48-hour PA-treated INS-1 cells (Figure 5B), indicative of reduced cell cycle progression. Furthermore, fivefold more annexin V-positive cells were observed in the PA-treated cultures as compared to vehicle-treated cultures (Figure 5C), suggesting elevated apoptosis in INS-1 cells exposed to PA for 48 hours. In addition, cleaved caspase 3, induced by PA treatment, correlated with down-regulation of AKT phosphorylation (Figure 5D). Together, these data indicate that prolonged exposure of beta-cells to PA leads to reduced cell cycle progression and induces cell death.

### Prolonged PA Exposure—Induced Phospho-AKT Involves Activation of p70S6K and Raptor/mTOR Complex

AKT1 plays an important role in the adaptive response of beta-cells to HFD.<sup>49</sup> The data here suggest that PA-regulated cell growth and survival are dependent on AKT phosphorylation, where suppression of phospho-AKT is concurrent with PA-induced beta-cell apoptosis and growth suppression. To explore how PA exposure leads to the down-regulation of AKT phosphorylation, the level of PTEN was determined, because beta-cell deletion of *Pten* results in improved beta-cell function and survival of beta-cells.<sup>36,37</sup> In either mEF or beta-cell lines, PTEN did not change in response to PA exposure (Figure 6A). In islets, PA treatment had a minor effect on PTEN expression (Figure 6A). Thus, it is unlikely that the down-regulation of AKT phosphorylation induced by PA occurs due to PTEN induction.

In order to explore the mechanisms by which chronic HFD exposure leads to reduced phospho-AKT, RNA-seq analysis was performed in islets from HFD fed mice

**B**

**Figure 2** Chronic high-fat diet–induced beta-cell apoptosis. **A:** Three-month–old mice were put on a high-fat diet (HFD) or normal chow (NC) for 9 and 14 months. Sections of pancreas were stained with insulin (red) and TUNEL (green). Blue, DAPI. **Arrows:** TUNEL-positive cells. **B:** Quantification of the TUNEL-stained islets in 14-month mice using ImageJ version 2.0 software.  $n = 5$ . Scale bar = 100  $\mu\text{m}$ .

(<https://www.ncbi.nlm.nih.gov/geo>; accession number GSE183778). The results demonstrate that mTOR/p70S6K is among the top three major signaling pathways induced in islets by HFD feeding (Supplemental Figure S1). Gene set enrichment analysis showed a significant up-regulation of mTOR signaling in islets isolated from the HFD-fed mice versus controls (Figure 6B). To confirm that mTOR signal is indeed induced even with down-regulation of AKT activity, S6K phosphorylation was studied in response to PA treatment. In mEFs exposed to PA for 24 and 18 hours, PA treatment induced phospho-S6K even though phospho-AKT was inhibited, particularly with 24 hour exposure (Figure 6C).

The same association of phospho-AKT and phospho-S6K was observed with beta-cells exposed to PA for 48 hours, concurrent with increased phosphorylation of mTOR-Ser2448 (Figure 6D). Similar induction of S6K and mTOR phosphorylation was observed in islets from mice fed HFD diet (Figure 6E). These data together suggest that prolonged lipid exposure, while inhibiting AKT activity, is inducing the activity of mTOR.

Although mTOR activation is often indicative of active AKT activity, it also serves as the kinase that phosphorylates AKT. In addition, chronic activation of mTOR signal is reported to induce a S6K-dependent phosphorylation of

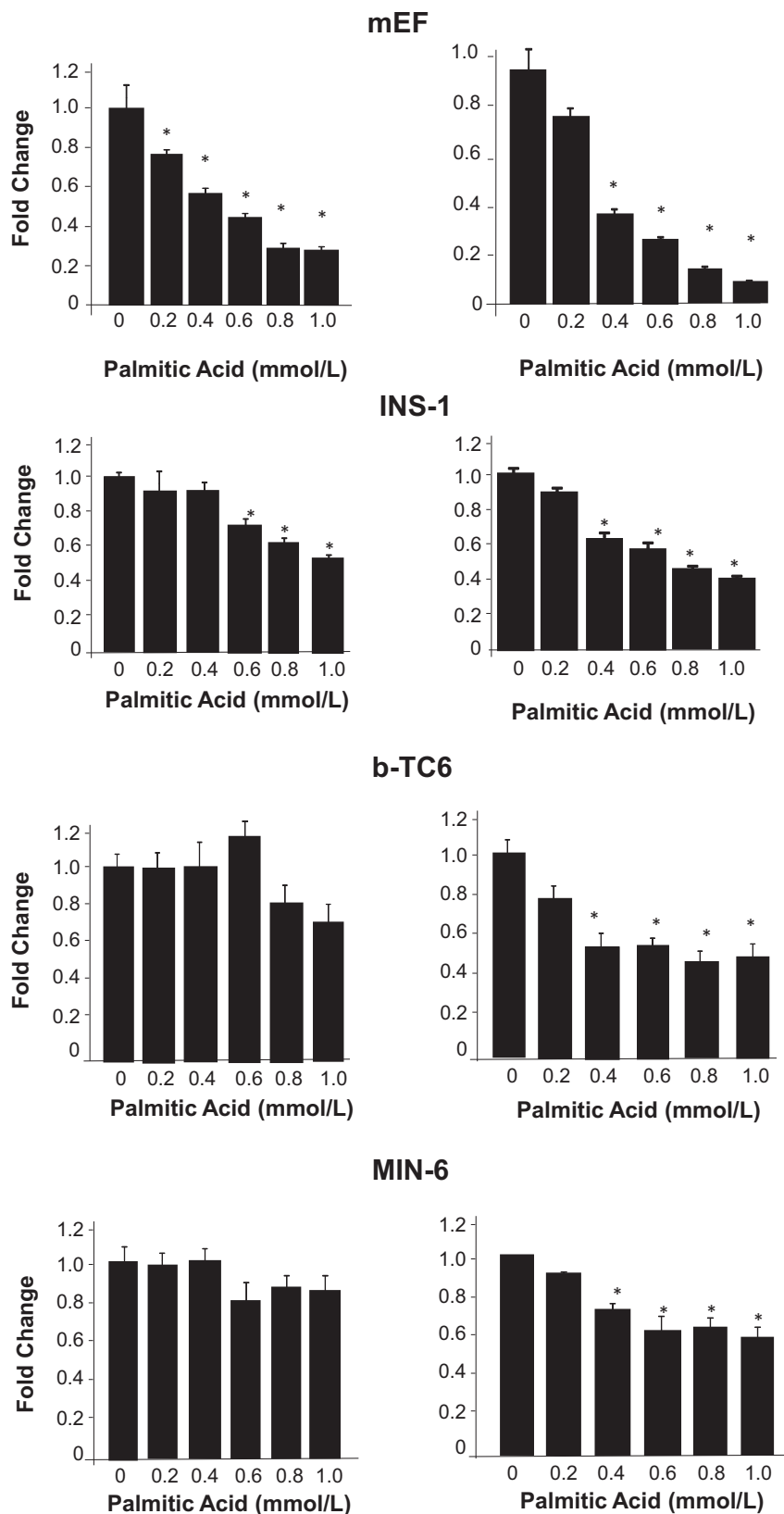


**Figure 3** Prolonged exposure to palmitic acid treatment reduces cell survival/growth in multiple cell lines. In mouse embryonic fibroblasts (mEF; **top row**), as well as three beta-cell cell lines (**bottom three rows**), exposure to palmitic acid for 24 hours (**left column**) and 48 hours (**right column**) induced loss of cell viability/growth potential as measured with MTT assay. Experiments were repeated multiple times.  $n = 3$ . \* $P < 0.05$  compared to vehicle-treated samples.



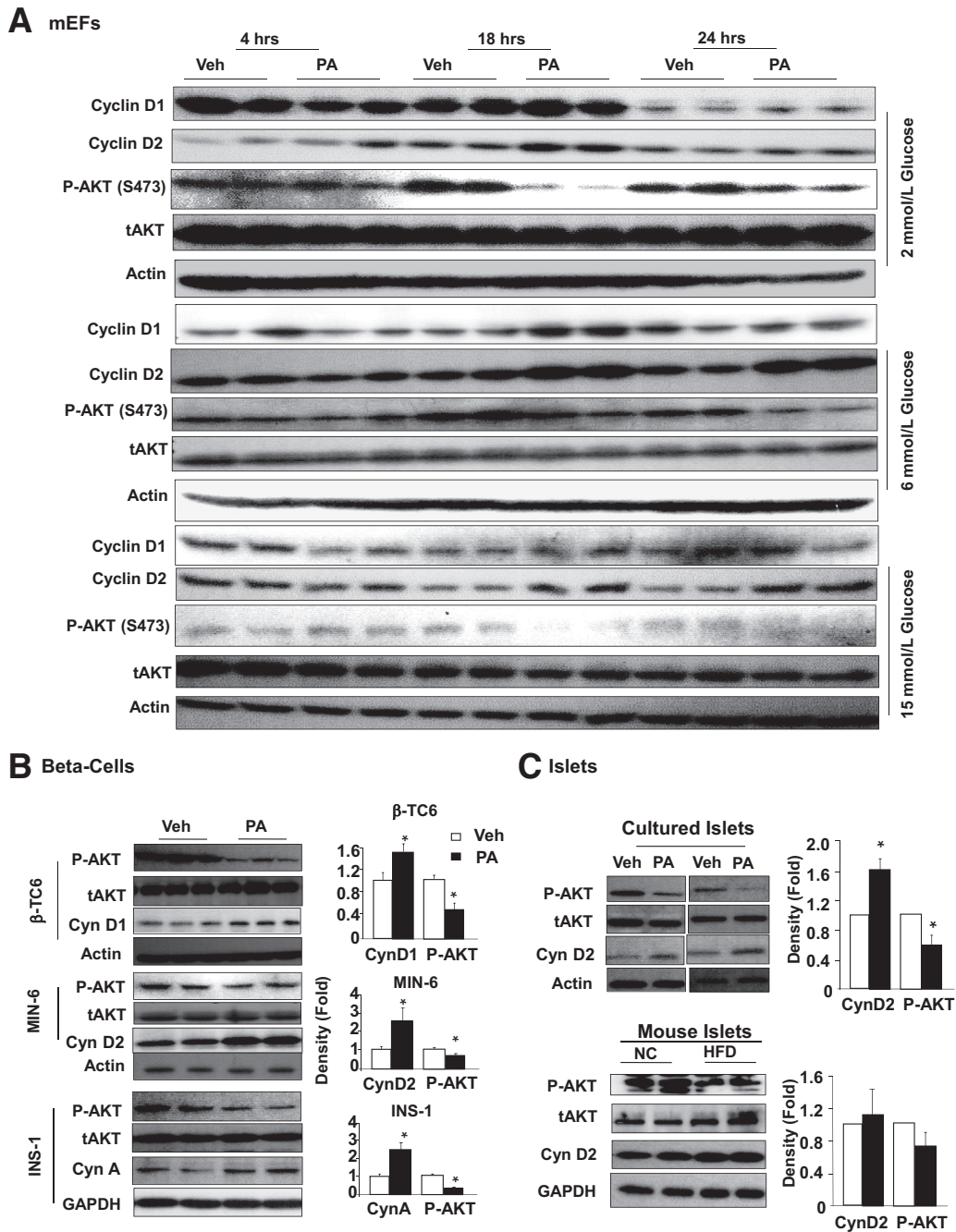


**Figure 4** Chronic exposure to palmitic acid treatment induces cell cyclin D2 expression while inhibiting AKT phosphorylation. **A:** Mouse embryonic fibroblasts (mEFs) were exposed to 0.4 mmol/L palmitic acid (PA) or dimethyl sulfoxide (DMSO; Veh) for indicated time points in the presence of indicated glucose concentrations. Cells were harvested and immunoblotting was performed for the indicated proteins. **B:** Three different beta-cell cell lines were exposed to 0.4 mmol/L PA for 48 hours in the presence of 6 mmol/L glucose. **Left panel**, immunoblotting for cyclins, phospho-AKT (P-AKT), and total AKT (tAKT) confirmed up-regulation of G1/S cyclins and down-regulation of phospho-AKT by PA treatment. Each lane represents an independent cell culture experiment. **Right panels**, densitometry quantification of the ratio of cyclins versus loading control and p-AKT versus tAKT. **C:** Top, isolated islets were cultured in the presence or absence of 0.4 mmol/L PA for 72 hours, and immunoblotting for P-AKT showed down-regulation of P-AKT by 0.4 mmol/L PA treatment. Each lane represents an independent islet culture experiment. Bottom, islets isolated from mice fed HFD for 4 months shows down-regulation of P-AKT. Each lane represents an independent mouse. Right, densitometry quantification of the ratio of cyclins versus loading control and p-AKT versus tAKT. *n* = 7 to 11 (**B**); *n* = 5 to 7 (**C**, top); *n* = 3 (**C**, bottom). \**P* < 0.05 compared to vehicle-treated samples.

IRS-1, serving as a feedback loop to inhibit AKT activity.<sup>56–58</sup> Consistently, phosphorylation of IRS-1 (Ser 1101) was observed, concurrent with the phosphorylation of S6K and mTOR in beta-cells (Figure 6D). To address

whether the PA-induced AKT down-regulation is dependent on this feedback loop, INS-1 cells were treated with rapamycin in combination with PA. As an inhibitor for mTOR activity, rapamycin treatment effectively inhibited

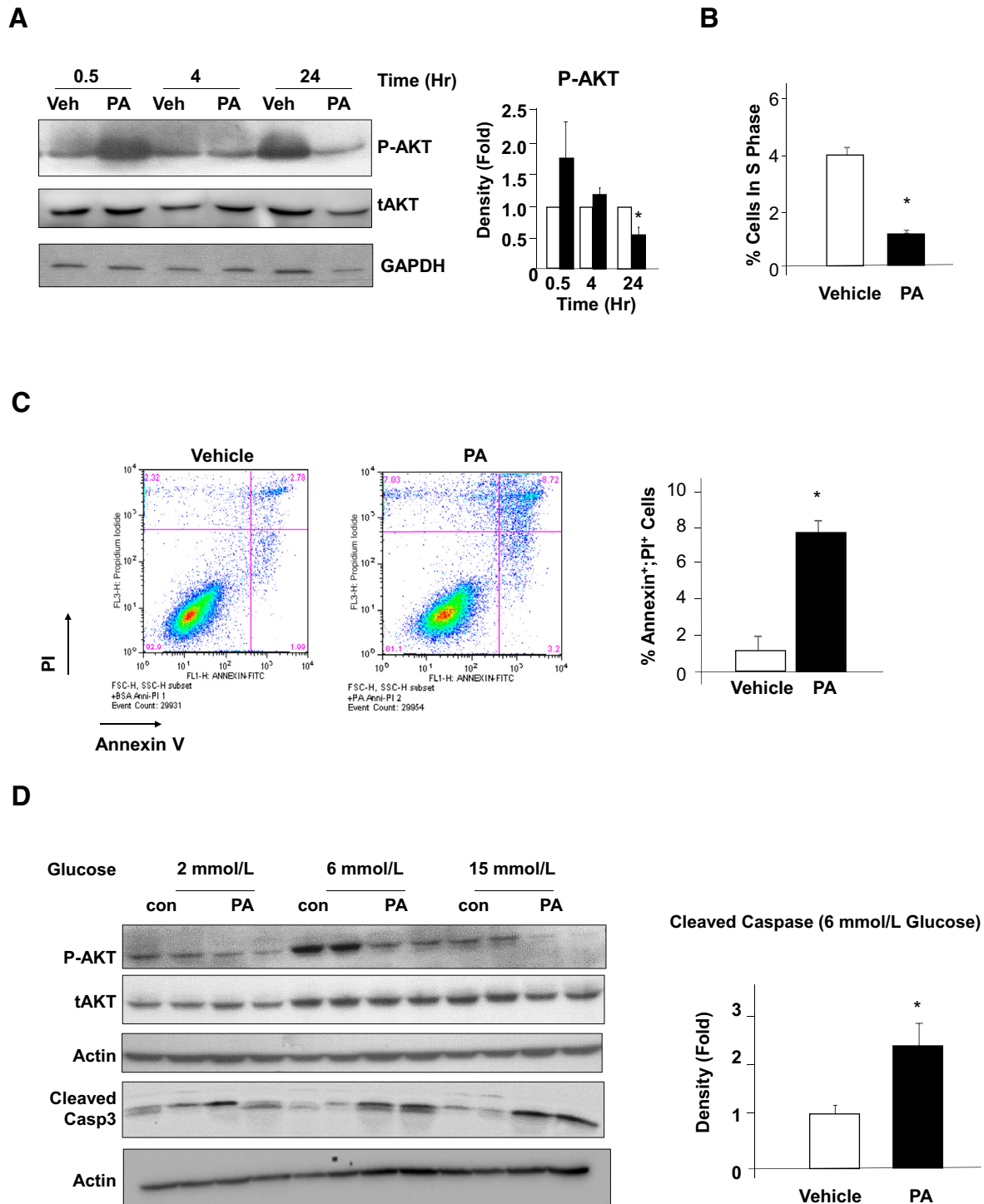


**Figure 5** Biphasic response of phospho-AKT to palmitic acid (PA) and regulation of beta-cell growth and apoptosis. **A:** Short-term exposure to 0.4 mmol/L PA reduced AKT phosphorylation, whereas prolonged exposure induced it. INS-1 cells were exposed to 0.4 mmol/L PA or dimethyl sulfoxide (DMSO; Veh) for the indicated time points in the presence of 6 mmol/L glucose. Left, immunoblotting is performed on lysates isolated from the cells for phospho-AKT (P-AKT) and total AKT (tAKT). Each lane represents an independent cell culture experiment. Right, densitometry quantification of the ratio of P-AKT versus tAKT. **B:** INS-1 cells were treated with 0.4 mmol/L PA for 48 hours followed by flow cytometry analysis for the cell cycle. Percentage of cells in S phase is reported here. Experiments were repeated multiple times. **C:** INS-1 cells treated with 0.4 mmol/L PA for 48 hours were stained with annexin V and propidium iodide (PI), and analyzed using flow cytometry (left and middle panels). Percentage of cells dual positive for annexin V and PI are reported in the right panel. Experiments were repeated multiple times. **D:** INS-1 cells treated with 0.4 mmol/L PA or DMSO (Veh) in the presence of a different amount of glucose were lysed and proteins blotted for P-AKT, tAKT, and cleaved caspase 3 with actin as loading control (left). Each lane represents an independent cell culture experiment. Right, densitometry quantification of the ratio of cleaved caspase 3 versus actin in 6 mmol/L glucose condition. Experiments were repeated multiple times.  $n = 3$ . \* $P < 0.05$  compared to vehicle-treated samples.

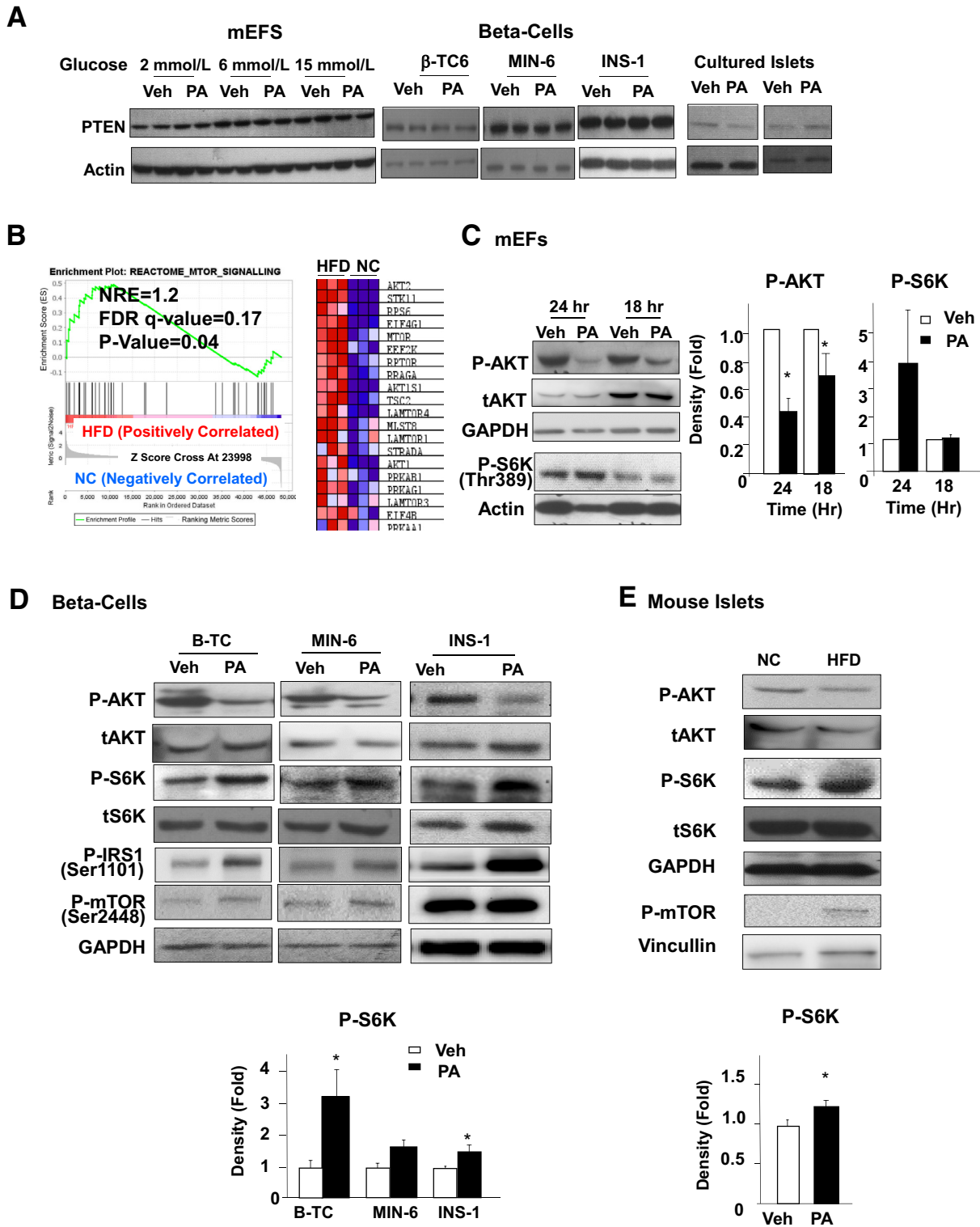


**Figure 6** S6K signal, but not PTEN, is altered by exposure to palmitic acid (PA). **A:** Mouse embryonic fibroblasts (mEF), beta-cells, and cultured islets treated with 0.4 mmol/L PA or dimethyl sulfoxide (DMSO; Veh) were lysed and analyzed for PTEN expression. Each lane represents an independent cell culture experiment. Experiment was repeated multiple times. **B:** Gene enrichment analysis of mTOR signal genes in islets from mice fed HFD for 4 months versus those fed normal chow (NC). **C:** mEF cells exposed to 0.4 mmol/L PA or vehicle with 6 mmol/L glucose were analyzed for phospho-AKT (p-AKT), total AKT (tAKT), and phospho-S6K (P-S6K). Each lane represents an independent cell culture experiment. **Right two panels,** densitometry quantification of the ratio of P-AKT versus tAKT, and S6K cyclins versus actin. **D and E:** Three beta-cell lines were treated with 0.4 mmol/L PA with 6 mmol/L glucose (**D**), and isolated islets from HFD (4 months) versus normal chow (NC) fed mice (**E**) were analyzed for P-AKT, tAKT, phospho-insulin receptor substrate 1 (P-IRS1), phospho-mTOR (P-mTOR), P-S6K, and total S6K (tS6K). Each lane represents an independent cell culture experiment or mouse. **Bottom panels,** densitometry quantification of the ratio of P-AKT versus tAKT. Experiments were repeated multiple times.  $n = 3$  (**B** and **C**);  $n = 5$  (**D** and **E**).  $*P < 0.05$  between PA- and vehicle-treated samples.

phosphorylation of S6K. The data indicated that the PA-induced down-regulation of AKT phosphorylation is readily rescued by rapamycin treatment (Figure 7A). These data suggest that the PA-regulated down-regulation of phospho-AKT is dependent on mTOR signaling. To address how PA may regulate mTOR signal, expression of Raptor and Rictor was studied. The data indicate that the overall protein levels of Raptor (but not Rictor) are increased with PA treatment (Figure 7B). Because activation of the Raptor-containing mTOR complex by nutrients leads to phosphorylation of S6K and subsequent inhibition of AKT via IRS-1 phosphorylation,<sup>44</sup> these data are consistent with the notion that the up-regulation of Raptor-containing mTOR complex by PA treatment is responsible for the S6K-dependent down-regulation of AKT phosphorylation.

## Discussion

Obesity, a major complication associated with T2D, increases the demand of insulin secretion to cope with hyperglycemia pressure.<sup>3</sup> The increased insulin secretion is accompanied by the increased proliferation of pancreatic beta-cells.<sup>2–6</sup> This enhanced growth response from beta-cells is followed by failure of beta-cells where both the mass and function of beta-cells decline when the demand for increased insulin output sustains for a chronic period of time.<sup>3,59,60</sup> In recent years, the ability of glucose to induce beta-cell replication has been established<sup>8,61</sup>; however, whether lipid induces beta-cell replication or promotes their apoptosis is still unclear. Studies focusing on the role of lipid or HFD suggest that short-term and low-dose exposure to lipid is likely pro-growth for beta-cells, whereas long-term and high-dose exposure results in the death of beta-cells.<sup>3,11,59,62–65</sup> However, the dynamics and mechanism by which lipid can induce both beta-cell growth and their apoptosis are not clear. The current study explored the dynamic response and mechanistic base for the lipid-induced beta-cell compensatory response and reports several major findings. First, the dynamics of beta-cell response to HFD feeding were determined. Beta-cell proliferation peaked at 2 months after initiation of HFD feeding, preceding the peaks in increased insulin secretion (4 months) and islet mass (9 months). Chronic exposure to HFD (14 months) resulted in reduction of beta-cell proliferation and elevated apoptosis. Second, cell culture models were established that mimic the biphasic response to chronic lipid exposure with multiple beta-cell cell lines. Using these model systems to confirm what was observed in mouse models, the study showed that chronic exposure (>4 hours) to PA leads to down-regulation of phospho-AKT, whereas short exposure (30 minutes) results in its induction. Third, down-regulation of phospho-AKT occurs simultaneously with increases in annexin V-positive apoptotic cells as well as reduction of cells in S phase. Fourth, down-regulation of phospho-AKT

by PA is not a result of altered expression of PTEN, but is regulated by Raptor-mTOR-mediated S6K activation.

A “beta-cell exhaust” idea has been proposed where rapid growth of beta-cells induced by HFD leads to exhaustion of their growth capacity resulting in failure.<sup>66</sup> The current study started by exploring the molecular signals induced by HFD that regulate beta-cell growth. Using PA treatment in cultured beta-cells and islets, the data demonstrated that chronic exposure to lipids leads to reduced viability and inhibition of cell cycle progression concurrent with down-regulation of a pro-growth/survival kinase AKT, independent of glucose. Genetic studies targeting AKT and signals regulating AKT have demonstrated a role for the AKT isoforms in the regulation of beta-cell growth/survival and islet mass.<sup>29,31,34,38,67–71</sup> AKT2 was found to be required for maintaining metabolic homeostasis as *Akt2*<sup>−/−</sup> mice develop insulin resistance, which indirectly leads to induced beta-cell mass due to adaptive beta-cell response.<sup>67</sup> The role of AKT1 in metabolic regulation lies in its ability to regulate the adaptive growth and survival of pancreatic beta-cells.<sup>49</sup> Mice deficient in AKT1 function display normal beta-cell mass and morphology,<sup>29,68</sup> whereas ectopic over-expression of constitutively active AKT1 in beta-cells leads to a dramatic increase in islet mass.<sup>31,34</sup> In addition, deletion of *Pten* in beta-cells, which leads to constitutive activation of AKT1, results in increased beta-cell proliferation, enhanced islet mass, and hypoglycemia in mice.<sup>36,37</sup> Consistently in beta-cells, AKT1 is indispensable for the adaptive growth response for beta-cells fed HFD.<sup>49</sup> Loss of AKT1 function induces mild endoplasmic reticulum stress and predisposes beta-cells to chronic HFD-induced cell death.<sup>49,53</sup>

In the past 2 decades, studies using genetically modified animals suggest a major role for the G1/S cell cycle machinery and key mitogenic signals such as IGF, platelet-derived growth factor (PDGF), and HGF in the growth of beta-cells.<sup>72</sup> Among the molecular signals that control beta-cell replication, genetic evidence targeting different signaling molecules confirmed the importance of PI3K signal downstream of the growth factors in the regulation of beta-cell replication. The negative regulator of this mitogenic signaling, PTEN, was previously shown to be induced by HFD feeding *in vivo* with unclear mechanisms.<sup>73</sup> Mice lacking PTEN specifically in the beta-cells have more and larger islets, and demonstrate a role of PTEN/PI3K signaling in beta-cell growth and senescence.<sup>33,35,36,53</sup> The current study shows that the PA-induced AKT down-regulation is not a result of induced expression of its negative regulator PTEN, but is due to the feedback regulatory loop mediated by mTOR. The data showed that chronic exposure of beta-cells and islets to PA results in concurrent activation of S6K and inhibition of AKT. This analysis suggests that the mTOR-AKT negative feedback loop signaling is induced by chronic exposure to lipids and that this feedback signal is likely responsible for the dipole response of beta-cells to lipid/HFD exposure (Figure 7C).

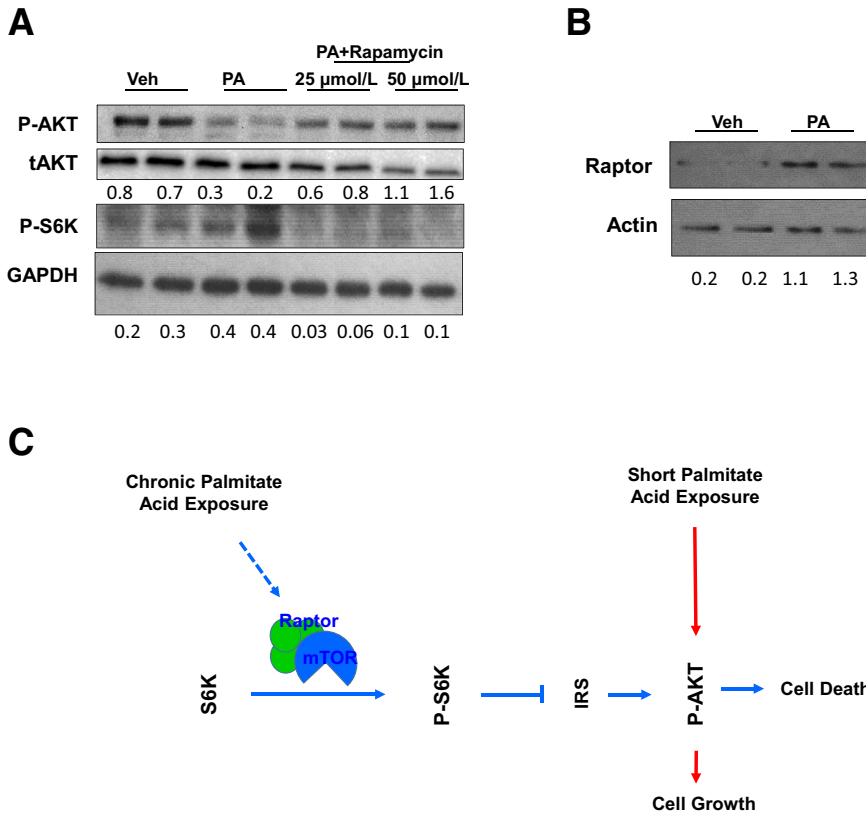


**Figure 7** Induction of mTOR-S6K leads to down-regulation of AKT phosphorylation due to exposure to palmitic acid (PA). **A:** INS-1 cells were treated with PA or PA+rapamycin and analyzed for phospho-AKT (P-AKT), total AKT (tAKT), and phospho-S6K (P-S6K). **B:** INS-1 cells treated with PA or vehicle (Veh) were analyzed for Raptor. **C:** Proposed role of palmitic acid on loss of beta-cell function via S6K-regulated AKT phosphorylation. Each lane represents an independent cell culture experiment or mouse. Densitometry quantification is provided for P-AKT/AKT, P-S6K/GAPDH, and Raptor/actin.

Though transient activation of mTOR leads to enhanced cell survival, chronic activation of mTOR results in inhibition of PI3K/AKT action via IRS and promotion of cell death.<sup>74</sup> Such feedback can block the action of PI3K and results in the down-regulation of downstream signaling molecules, including Ser/Thr kinase AKT.<sup>75</sup> Consistently, mice lacking either TSC1 or TSC2 (with activated mTOR signal) in beta-cells display beta-cell failure with reduced islet mass and function, and develop diabetes-like phenotypes when they get older.<sup>40</sup> Such failure is mediated by the activation of mTOR because rapamycin treatment to inhibit mTOR activity can rescue the failure of beta-cells in these mice.<sup>40</sup> Interestingly, the rapamycin treatment also induced the phosphorylation of AKT.

The mTOR kinase exists in two separate complexes with other regulatory factors.<sup>74</sup> Previous studies have reported that Myc-dependent adaptive response to glucose is regulated by the TORC1 mTOR complex.<sup>76</sup> The TORC1 complex is composed of Raptor and PRAS40. TORC1 complex phosphorylates and activates S6K, which phosphorylates and inactivates IRS1/2. The TORC2 complex is composed of Rictor, mSin1, and Protor. Chronic activation of mTOR also leads to TORC2-induced phosphorylation and degradation of IRS1/2. The current data demonstrated a consistent activation of S6K phosphorylation in response to lipid treatment. These data suggest that lipid treatment at least activates the TORC1 complex, an observation confirmed by

the up-regulation of Raptor. In experimental models, loss of mTORC1 signal also leads to beta-cell failure and results in diabetes phenotypes.<sup>38</sup> However, inhibition of S6K leads to improved glucose-induced insulin secretion in isolated human islets.<sup>41</sup> Thus, further exploration into the mTOR-S6K-AKT is needed to understand the dynamics of response of this signaling axis and lipid exposure. Particularly, understanding the mechanisms by which lipid exposure regulates mTOR signaling is necessary, not only for elucidating the adaptive response of beta-cells to lipid exposure, but also for other cell growth responses to dyslipidemia. A putative mechanism characterized for lipid-mTOR interaction impinges on phosphatidyl acid.<sup>77,78</sup> Binding of phosphatidic acid to the FRB domain of mTOR blocks binding of Deptor,<sup>79</sup> a partner of both TORC1 and TORC2 complex. Although initial immunoprecipitation in INS-1 cells did not confirm that PA treatment altered binding of Deptor to TORCs (data not shown), the current data show that total levels of Raptor are induced by PA treatment in INS-1 cells. Raptor is a component of the TORC1 complex, and elevated Raptor is consistent with the observed increase of phospho-S6K in response to PA treatment.

Together, the data suggest that Raptor-mTOR may act as a lipid sensor for HFD, and increased lipid levels can induce beta-cell proliferation followed by beta-cell failure due to the mTOR feedback loop. Induction of Raptor expression

and activation of S6K mediated down-regulation of AKT due to chronic exposure to lipids. The down-regulated AKT signal led to loss of growth potential and increased beta-cell death, leading to beta-cell failure in response to chronic lipid exposure. An increased activation of S6K has been recently reported in islets of human T2D patients where hyperlipidemia is common.<sup>41</sup> In these islets from T2D patients and db/db mice, inhibition of mTORC-S6K signal can indeed improve glucose-induced insulin secretion.<sup>41</sup> The current study showed that the mTOR feedback loop mediates the dipole effect of HFD and lipid-induced beta-cell growth deficiency, and it may be targeted to overcome beta-cell failure.

## Author Contributions

R.A. wrote the manuscript and conducted experiments; Z.P., N.Z., J.S., L.H., J.C., A.D., and C.-Y.C. conducted experiments; T.T., M.A., E.X.S., and H. H analyzed image quantification; B.L.S. directed the project, and wrote and edited the manuscript.

## Supplemental Data

Supplemental material for this article can be found at <http://doi.org/10.1016/j.ajpath.2021.09.008>.

## References

- Buchanan TA: Pancreatic beta-cell loss and preservation in type 2 diabetes. *Clin Ther* 2003, 25(Suppl B):B32–B46
- Gonzalez A, Merino B, Marroquí L, Neco P, Alonso-Magdalena P, Caballero-Garrido E, Vieira E, Soriano S, Gomis R, Nadal A, Quesada I: Insulin hypersecretion in islets from diet-induced hyperinsulinemic obese female mice is associated with several functional adaptations in individual beta-cells. *Endocrinology* 2013, 154: 3515–3524
- Stamateris RE, Sharma RB, Hollern DA, Alonso LC: Adaptive beta-cell proliferation increases early in high-fat feeding in mice, concurrent with metabolic changes, with induction of islet cyclin D2 expression. *Am J Physiol Endocrinol Metab* 2013, 305:E149–E159
- Surwit RS, Kuhn CM, Cochrane C, McCubbin JA, Feinglos MN: Diet-induced type II diabetes in C57BL/6J mice. *Diabetes* 1988, 37: 1163–1167
- Tomita T: Apoptosis in pancreatic beta-islet cells in type 2 diabetes. *Bosn J Basic Med Sci* 2016, 16:162–179
- Winzell MS, Ahrén B: The high-fat diet-fed mouse: a model for studying mechanisms and treatment of impaired glucose tolerance and type 2 diabetes. *Diabetes* 2004, 53(Suppl 3):S215–S219
- O'Brien T, Nguyen TT, Zimmerman BR: Hyperlipidemia and diabetes mellitus. *Mayo Clin Proc* 1998, 73:969–976
- Salpeter SJ, Klochendler A, Weinberg-Corem N, Porat S, Granot Z, Shapiro AMJ, Magnuson MA, Eden A, Grimsby J, Glaser B, Dor Y: Glucose regulates cyclin D2 expression in quiescent and replicating pancreatic beta-cells through glycolysis and calcium channels. *Endocrinology* 2011, 152:2589–2598
- Stamateris RE, Sharma RB, Kong Y, Ebrahimpour P, Panday D, Ranganath P, Zou B, Levitt H, Parambil NA, O'Donnell CP, García-Ocaña A, Alonso LC: Glucose induces mouse beta-cell proliferation via IRS2, MTOR, and cyclin D2 but not the insulin receptor. *Diabetes* 2016, 65:981–995
- Collins SC, Salehi A, Eliasson L, Olofsson CS, Rorsman P: Long-term exposure of mouse pancreatic islets to oleate or palmitate results in reduced glucose-induced somatostatin and oversecretion of glucagon. *Diabetologia* 2008, 51:1689–1693
- Maedler K, Oberholzer J, Bucher P, Spinass GA, Donath MY: Monounsaturated fatty acids prevent the deleterious effects of palmitate and high glucose on human pancreatic beta-cell turnover and function. *Diabetes* 2003, 52:726–733
- Moullé VS, Vivot K, Tremblay C, Zarrouki B, Ghislain J, Poirout V: Glucose and fatty acids synergistically and reversibly promote beta cell proliferation in rats. *Diabetologia* 2017, 60:879–888
- Poirout V, Amyot J, Semache M, Zarrouki B, Hagman D, Fontés G: Glucolipotoxicity of the pancreatic beta cell. *Biochim Biophys Acta* 2010, 1801:289–298
- Wang Y, Wang P-Y, Takashi K: Chronic effects of different non-esterified fatty acids on pancreatic islets of rats. *Endocrine* 2006, 29:169–173
- Ayvaz G, Balos Törtüner F, Karakoç A, Yetkin I, Cakir N, Arslan M: Acute and chronic effects of different concentrations of free fatty acids on the insulin secreting function of islets. *Diabetes Metab* 2002, 28(Pt 5):3S7–3S12. discussion 3S108–3S112
- Lupi R, Dotta F, Marselli L, Del Guerra S, Masini M, Santangelo C, Patané G, Boggi U, Piro S, Anello M, Bergamini E, Mosca F, Di Mario U, Del Prato S, Marchetti P: Prolonged exposure to free fatty acids has cytostatic and pro-apoptotic effects on human pancreatic islets: evidence that beta-cell death is caspase mediated, partially dependent on ceramide pathway, and Bcl-2 regulated. *Diabetes* 2002, 51:1437–1442
- Oprescu AI, Bikopoulos G, Naassan A, Allister EM, Tang C, Park E, Uchino H, Lewis GF, Fantus IG, Rozakis-Adcock M, Wheeler MB, Giacca A: Free fatty acid-induced reduction in glucose-stimulated insulin secretion: evidence for a role of oxidative stress in vitro and in vivo. *Diabetes* 2007, 56:2927–2937
- Zhou YP, Grill VE: Long-term exposure of rat pancreatic islets to fatty acids inhibits glucose-induced insulin secretion and biosynthesis through a glucose fatty acid cycle. *J Clin Invest* 1994, 93:870–876
- Brelje TC, Bhagroo NV, Stout LE, Sorenson RL: Beneficial effects of lipids and prolactin on insulin secretion and beta-cell proliferation: a role for lipids in the adaptation of islets to pregnancy. *J Endocrinol* 2008, 197:265–276
- Hosokawa H, Corkey BE, Leahy JL: Beta-cell hypersensitivity to glucose following 24-h exposure of rat islets to fatty acids. *Diabetologia* 1997, 40:392–397
- Milburn JL Jr, Hirose H, Lee YH, Nagasawa Y, Ogawa A, Ohneda M, BeltrandelRio H, Newgard CB, Johnson JH, Unger RH: Pancreatic beta-cells in obesity. Evidence for induction of functional, morphologic, and metabolic abnormalities by increased long chain fatty acids. *J Biol Chem* 1995, 270:1295–1299
- Mellado-Gil J, Rosa TC, Demirci C, Gonzalez-Pertusa JA, Velazquez-García S, Ernst S, Valle S, Vasavada RC, Stewart AF, Alonso LC, García-Ocaña A: Disruption of hepatocyte growth factor/c-Met signaling enhances pancreatic beta-cell death and accelerates the onset of diabetes. *Diabetes* 2011, 60:525–536
- Dai C, Huh CG, Thorgeirsson SS, Liu Y: Beta-cell-specific ablation of the hepatocyte growth factor receptor results in reduced islet size, impaired insulin secretion, and glucose intolerance. *Am J Pathol* 2005, 167:429–436
- Roccisana J, Reddy V, Vasavada RC, Gonzalez-Pertusa JA, Magnuson MA, García-Ocaña A: Targeted inactivation of hepatocyte growth factor receptor c-met in beta-cells leads to defective insulin secretion and GLUT-2 downregulation without alteration of beta-cell mass. *Diabetes* 2005, 54:2090–2102
- Dai C, Li Y, Yang J, Liu Y: Hepatocyte growth factor preserves beta cell mass and mitigates hyperglycemia in streptozotocin-induced diabetic mice. *J Biol Chem* 2003, 278:27080–27087

26. García-Ocaña A, Vasavada RC, Cebrian A, Reddy V, Takane KK, López-Talavera JC, Stewart AF: Transgenic overexpression of hepatocyte growth factor in the beta-cell markedly improves islet function and islet transplant outcomes in mice. *Diabetes* 2001, 50:2752–2762
27. García-Ocaña A, Takane KK, Syed MA, Philbrick WM, Vasavada RC, Stewart AF: Hepatocyte growth factor overexpression in the islet of transgenic mice increases beta cell proliferation, enhances islet mass, and induces mild hypoglycemia. *J Biol Chem* 2000, 275:1226–1232
28. Vila MR, Nakamura T, Real FX: Hepatocyte growth factor is a potent mitogen for normal human pancreas cells in vitro. *Lab Invest* 1995, 73:409–418
29. Bernal-Mizrachi E, Fatrai S, Johnson JD, Ohsugi M, Otani K, Han Z, Polonsky KS, Permutt MA: Defective insulin secretion and increased susceptibility to experimental diabetes are induced by reduced Akt activity in pancreatic islet beta cells. *J Clin Invest* 2004, 114:928–936
30. Liu W, Chin-Chance C, Lee EJ, Lowe WL Jr: Activation of phosphatidylinositol 3-kinase contributes to insulin-like growth factor I-mediated inhibition of pancreatic beta-cell death. *Endocrinology* 2002, 143:3802–3812
31. Tuttle RL, Gill NS, Pugh W, Lee JP, Koeberlein B, Furth EE, Polonsky KS, Naji A, Bimbaum MJ: Regulation of pancreatic beta-cell growth and survival by the serine/threonine protein kinase Akt1/PKBalpha. *Nat Med* 2001, 7:1133–1137
32. Holst LS, Mulder H, Manganiello V, Sundler F, Ahrén B, Holm C, Degerman E: Protein kinase B is expressed in pancreatic beta cells and activated upon stimulation with insulin-like growth factor I. *Biochem Biophys Res Commun* 1998, 250:181–186
33. Bayan JA, Peng Z, Zeng N, He L, Chen J, Stiles BL: Crosstalk between activated myofibroblasts and beta cells in injured mouse pancreas. *Pancreas* 2015, 44:1111–1120
34. Bernal-Mizrachi E, Wen W, Stahlhut S, Welling CM, Permutt MA: Islet beta cell expression of constitutively active Akt1/PKB alpha induces striking hypertrophy, hyperplasia, and hyperinsulinemia. *J Clin Invest* 2001, 108:1631–1638
35. Stiles BL, Kuralwalla-Martinez C, Guo W, Gregorian C, Wang Y, Tian J, Magnuson MA, Wu H: Selective deletion of Pten in pancreatic beta cells leads to increased islet mass and resistance to STZ-induced diabetes. *Mol Cell Biol* 2006, 26:2772–2781
36. Yang KT, Bayan JA, Zeng N, Aggarwal R, He L, Peng Z, Kassa A, Kim M, Luo Z, Shi Z, Medina V, Boddupally K, Stiles BL: Adult-onset deletion of Pten increases islet mass and beta cell proliferation in mice. *Diabetologia* 2014, 57:352–361
37. Zeng N, Yang KT, Bayan JA, He L, Aggarwal R, Stiles JW, Hou X, Medina V, Abad D, Palian BM, Al-Abdullah I, Kandeel F, Johnson DL, Stiles BL: PTEN controls beta-cell regeneration in aged mice by regulating cell cycle inhibitor p16ink4a. *Aging Cell* 2013, 12:1000–1011
38. Blandino-Rosano M, Barbaresso R, Jimenez-Palomares M, Bozadjieva N, Werneck-de-Castro JP, Hatanaka M, Mirmira RG, Sonenberg N, Liu M, Rüegg MA, Hall MN, Bernal-Mizrachi E: Loss of mTORC1 signalling impairs beta-cell homeostasis and insulin processing. *Nat Commun* 2017, 8:16014
39. Helman A, Klochendler A, Azazmeh N, Gabai Y, Horwitz E, Anzi S, Swisa A, Condiotti R, Granit RZ, Nevo Y, Fixler Y, Shreibman D, Zamir A, Tornovsky-Babeay S, Dai C, Glaser B, Powers AC, Shapiro AM, Magnuson MA, Dor Y, Ben-Porath I: p16(Ink4a)-induced senescence of pancreatic beta cells enhances insulin secretion. *Nat Med* 2016, 22:412–420
40. Shigeyama Y, Kobayashi T, Kido Y, Hashimoto N, Asahara S-I, Matsuda T, Takeda A, Inoue T, Shibutani Y, Koyanagi M, Uchida T, Inoue M, Hino O, Kasuga M, Noda T: Biphasic response of pancreatic beta-cell mass to ablation of tuberous sclerosis complex 2 in mice. *Mol Cell Biol* 2008, 28:2971–2979
41. Yuan T, Rafizadeh S, Gorrepati KD, Lupse B, Oberholzer J, Maedler K, Ardestani A: Reciprocal regulation of mTOR complexes in pancreatic islets from humans with type 2 diabetes. *Diabetologia* 2017, 60:668–678
42. Kwon G, Marshall CA, Pappan KL, Remedi MS, McDaniel ML: Signaling elements involved in the metabolic regulation of mTOR by nutrients, incretins, and growth factors in islets. *Diabetes* 2004, 53(Suppl 3):S225–S232
43. Shah OJ, Hunter T: Turnover of the active fraction of IRS1 involves raptor-mTOR- and S6K1-dependent serine phosphorylation in cell culture models of tuberous sclerosis. *Mol Cell Biol* 2006, 26:6425–6434
44. Tzatsos A, Kandror KV: Nutrients suppress phosphatidylinositol 3-kinase/Akt signaling via raptor-dependent mTOR-mediated insulin receptor substrate 1 phosphorylation. *Mol Cell Biol* 2006, 26:63–76
45. Chen C-Y, Li Y, Zeng N, He L, Zhang X, Tu T, Tang Q, Alba M, Mir S, Stiles EX, Hong H, Cadenas E, Stolz AA, Li G, Stiles BL: Inhibition of estrogen-related receptor alpha blocks liver steatosis and steatohepatitis and attenuates triglyceride biosynthesis. *Am J Pathol* 2021, 191:1240–1254
46. Chen J, Debebe A, Zeng N, Kopp J, He L, Sander M, Stiles BL: Transformation of SOX9(+) cells by Pten deletion synergizes with steatotic liver injury to drive development of hepatocellular and cholangiocarcinoma. *Sci Rep* 2021, 11:11823
47. Debebe A, Medina V, Chen CY, Mahajan IM, Jia C, Fu D, He L, Zeng N, Stiles BW, Chen CL, Wang M, Aggarwal KR, Peng Z, Huang J, Chen J, Li M, Dong T, Atkins S, Borok Z, Yuan W, Machida K, Ju C, Kahn M, Johnson D, Stiles BL: Wnt/beta-catenin activation and macrophage induction during liver cancer development following steatosis. *Oncogene* 2017, 36:6020–6029
48. He L, Li Y, Zeng N, Stiles BL: Regulation of basal expression of hepatic PEPCK and G6Pase by AKT2. *Biochem J* 2020, 477:1021–1031
49. Peng Z, Aggarwal R, Zeng N, He L, Stiles EX, Debebe A, Chen J, Chen CY, Stiles BL: AKT1 regulates endoplasmic reticulum stress and mediates the adaptive response of pancreatic beta cells. *Mol Cell Biol* 2020, 40:e00031-20
50. Jia C, Medina V, Liu C, He L, Qian D, Taojian T, Okamoto CT, Stiles BL: Crosstalk of LKB1- and PTEN-regulated signals in liver morphogenesis and tumor development. *Hepatol Commun* 2017, 1:153–167
51. Galicia VA, He L, Dang H, Kanel G, Vendryes C, French BA, Zeng N, Bayan JA, Ding W, Wang KS, French S, Birnbaum MJ, Rountree CB, Stiles BL: Expansion of hepatic tumor progenitor cells in Pten-null mice requires liver injury and is reversed by loss of AKT2. *Gastroenterology* 2010, 139:2170–2182
52. He L, Gubbins J, Peng Z, Medina V, Fei F, Asahina K, Wang J, Kahn M, Rountree CB, Stiles BL: Activation of hepatic stellate cell in Pten null liver injury model. *Fibrogenesis Tissue Repair* 2016, 9:8
53. Zeng N, Li Y, He L, Xu X, Galicia V, Deng C, Stiles BL: Adaptive basal phosphorylation of eIF2alpha is responsible for resistance to cellular stress-induced cell death in Pten-null hepatocytes. *Mol Cancer Res* 2011, 9:1708–1717
54. Li C, Li Y, He L, Agarwal AR, Zeng N, Cadenas E, Stiles BL: PI3K/AKT signaling regulates bioenergetics in immortalized hepatocytes. *Free Radic Biol Med* 2013, 60:29–40
55. Li Y, He L, Zeng N, Sahu D, Cadenas E, Shearn C, Li W, Stiles BL: Phosphatase and tensin homolog deleted on chromosome 10 (PTEN) signaling regulates mitochondrial biogenesis and respiration via estrogen-related receptor alpha (ERRalpha). *J Biol Chem* 2013, 288:25007–25024
56. Shah OJ, Wang Z, Hunter T: Inappropriate activation of the TSC/Rheb/mTOR/S6K cassette induces IRS1/2 depletion, insulin resistance, and cell survival deficiencies. *Curr Biol* 2004, 14:1650–1656
57. Tu T, Chen J, Chen L, Stiles BL: Dual-specific protein and lipid phosphatase PTEN and its biological functions. *Cold Spring Harb Perspect Med* 2020, 10:a036301

58. Vernier S, Chiu A, Schober J, Weber T, Nguyen P, Luer M, McPherson T, Wanda PE, Marshall CA, Rohatgi N, McDaniel ML, Greenberg AS, Kwon G: beta-Cell metabolic alterations under chronic nutrient overload in rat and human islets. *Islets* 2012, 4: 379–392
59. Mosser RE, Maulis MF, Moullé VS, Dunn JC, Carboneau BA, Arasi K, Pappan K, Poitout V, Gannon M: High-fat diet-induced beta-cell proliferation occurs prior to insulin resistance in C57Bl/6J male mice. *Am J Physiol Endocrinol Metab* 2015, 308:E573–E582
60. Potter KJ, Westwell-Roper CY, Klimek-Abercrombie AM, Warnock GL, Verchere CB: Death and dysfunction of transplanted beta-cells: lessons learned from type 2 diabetes? *Diabetes* 2014, 63: 12–19
61. Porat S, Weinberg-Corem N, Tornovsky-Babaey S, Schyr-Ben-Haroush R, Hija A, Stolovich-Rain M, Dadon D, Granot Z, Ben-Hur V, White P, Girard CA, Karni R, Kaestner KH, Ashcroft FM, Magnuson MA, Saada A, Grimsby J, Glaser B, Dor Y: Control of pancreatic beta cell regeneration by glucose metabolism. *Cell Metab* 2011, 13:440–449
62. El Ouaamari A, Zhou JY, Liew CW, Shirakawa J, Dirice E, Gedeon N, Kahraman S, De Jesus DF, Bhatt S, Kim JS, Clauss TR, Camp DG 2nd, Smith RD, Qian WJ, Kulkarni RN: Compensatory islet response to insulin resistance revealed by quantitative proteomics. *J Proteome Res* 2015, 14:3111–3122
63. Higa M, Shimabukuro M, Shimajiri Y, Takasu N, Shinjyo T, Inaba T: Protein kinase B/Akt signalling is required for palmitate-induced beta-cell lipotoxicity. *Diabetes Obes Metab* 2006, 8:228–233
64. Maedler K, Spinas GA, Dyntar D, Moritz W, Kaiser N, Donath MY: Distinct effects of saturated and monounsaturated fatty acids on beta-cell turnover and function. *Diabetes* 2001, 50:69–76
65. Roche E, Buteau J, Aniento I, Reig JA, Soria B, Prentki M: Palmitate and oleate induce the immediate-early response genes c-fos and nur-77 in the pancreatic beta-cell line INS-1. *Diabetes* 1999, 48: 2007–2014
66. Purrello F, Rabuazzo AM: Metabolic factors that affect beta-cell function and survival. *Diabetes Nutr Metab* 2000, 13:84–91
67. Cho H, Mu J, Kim JK, Thorvaldsen JL, Chu Q, Crenshaw EB 3rd, Kaestner KH, Bartolomei MS, Shulman GI, Birnbaum MJ: Insulin resistance and a diabetes mellitus-like syndrome in mice lacking the protein kinase Akt2 (PKB beta). *Science* 2001, 292: 1728–1731
68. Cho H, Thorvaldsen JL, Chu Q, Feng F, Birnbaum MJ: Akt1/PKB-Balpa is required for normal growth but dispensable for maintenance of glucose homeostasis in mice. *J Biol Chem* 2001, 276: 38349–38352
69. Leavens KF, Easton RM, Shulman GI, Previs SF, Birnbaum MJ: Akt2 is required for hepatic lipid accumulation in models of insulin resistance. *Cell Metab* 2009, 10:405–418
70. Treins C, Alliouachene S, Hassouna R, Xie Y, Birnbaum MJ, Pende M: The combined deletion of S6K1 and Akt2 deteriorates glycemic control in a high-fat diet. *Mol Cell Biol* 2012, 32:4001–4011
71. Zeng N, Bayan JA, He L, Stiles B: The role of PTEN in beta-cell growth. *Open Endocrinol J* 2010, 4:23–32
72. Stewart AF, Hussain MA, García-Ocaña A, Vasavada RC, Bhushan A, Bernal-Mizrachi E, Kulkarni RN: Human beta-cell proliferation and intracellular signaling: part 3. *Diabetes* 2015, 64: 1872–1885
73. Wang L, Liu Y, Yan Lu S, Nguyen K-T, Schroer SA, Suzuki A, Mak TW, Gaisano H, Woo M: Deletion of Pten in pancreatic beta-cells protects against deficient beta-cell mass and function in mouse models of type 2 diabetes. *Diabetes* 2010, 59:3117–3126
74. Saxton RA, Sabatini DM: mTOR signaling in growth, metabolism, and disease. *Cell* 2017, 168:960–976
75. Jhanwar-Uniyal M, Amin AG, Cooper JB, Das K, Schmidt MH, Murali R: Discrete signaling mechanisms of mTORC1 and mTORC2: connected yet apart in cellular and molecular aspects. *Adv Biol Regul* 2017, 64:39–48
76. Rosselot C, Kumar A, Lakshmi pathi J, Zhang P, Lu G, Katz LS, Prochownik EV, Stewart AF, Lambertini L, Scott DK, García-Ocaña A: Myc is required for adaptive beta-cell replication in young mice but is not sufficient in one-year-old mice fed with a high-fat diet. *Diabetes* 2019, 68:1934–1949
77. Fang Y, Vilella-Bach M, Bachmann R, Flanigan A, Chen J: Phosphatidic acid-mediated mitogenic activation of mTOR signaling. *Science* 2001, 294:1942–1945
78. Menon D, Salloum D, Bernfeld E, Gorodetsky E, Akselrod A, Frias MA, Sudderth J, Chen PH, DeBerardinis R, Foster DA: Lipid sensing by mTOR complexes via de novo synthesis of phosphatidic acid. *J Biol Chem* 2017, 292:6303–6311
79. Yoon M-S, Rosenberger CL, Wu C, Truong N, Sweedler JV, Chen J: Rapid mitogenic regulation of the mTORC1 inhibitor, DEPTOR, by phosphatidic acid. *Mol Cell* 2015, 58:549–556